DALTON

Raman spectroelectrochemical studies and crystal structure of a binuclear copper(I) complex with a bridging diimine ligand†

Keith C. Gordon, Ala H. R. Al-Obaidi, Pradeep M. Jayaweera, John J. McGarvey,* John F. Malone and Steven E. J. Bell

School of Chemistry, Queen's University of Belfast, Belfast BT9 5AG, UK

Raman spectroelectrochemical and X-ray crystallographic studies have been made for the binuclear copper(I) complex, $[(Ph_3P)_2Cu(dpq)Cu(PPh_3)_2][BF_4]_2$, where dpq is the bridging ligand 2,3-di(2-pyridyl)quinoxaline. The X-ray data show that the pyridine rings are twisted out of plane with respect to the quinoxaline ring which is itself non-planar. The UV/VIS spectra of the metal-to-ligand charge-transfer excited state and those of the electrochemically reduced complex are similar. The resonance-Raman spectrum of the latter species exhibits little change in the frequency of the pyridinylquinoxaline inter-ring C–C bond stretching mode, compared to the ground electronic state. This suggests minimum change in the inter-ring C–C bond order in the electrochemically or charge-transfer generated radical anion. Semiempirical molecular-orbital calculations on both the neutral dpq and radical anion show two near-degenerate lowest unoccupied orbitals in the neutral species. One is strongly bonding across the inter-ring C–C bond while the other is almost non-bonding. The Raman data suggest that it is this latter orbital which is populated in the transient and electrochemical experiments.

The photophysical and spectroelectrochemical properties of copper(I) complexes with diimine ligands are topics of developing interest. The luminescent properties of a range of mononuclear copper(I) systems have been studied extensively by McMillin *et al.*[1] Transient resonance-Raman spectroscopy has also been employed to explore the nature of the lowest-energy metal-to-ligand charge-transfer (m.l.c.t.) excited states of several systems.[2] The synthesis, spectroscopy and electrochemistry of a series of binuclear copper(I) complexes with polypyrazine bridging ligands have recently been reported.[3] One of the binuclear complexes listed in the latter work, $[(Ph_3P)_2Cu(dpq)Cu(PPh_3)_2][BF_4]_2$ **1** [dpq = 2,3-di(2-pyridyl)-quinoxaline], had previously been reported by ourselves some years ago[4] in a paper which described the flash photolysis and transient, power-resolved resonance-Raman spectroscopy of the species. Evidence was presented for the mixed-valence nature of the lowest-energy m.l.c.t. excited state which was shown to have a lifetime less than the duration of the laser pulse (*ca.* 8 ns). The conclusions were based on the growth of Raman bands with increasing laser power, similar to those observed for the corresponding mononuclear complex, $[Cu(PPh_3)_2(dpq)]^+$ **2**. The transient Raman spectra were attributed to the radical anion of the dpq bridging ligand.

We have now carried out a study of the spectroelectrochemistry of complex **1** using an optically transparent thin-layer electrode (OTTLE) cell and a complementary study of the resonance-Raman spectroscopy of the radical anion of **1** in order to provide independent support for the earlier conclusions. X-Ray crystallographic data for **1** are also presented. Semiempirical molecular orbital calculations have been carried out for the neutral dpq and the radical anion.

Experimental

Complexes **1** and **2** were prepared as described previously.[4]

Cyclic voltammetry (CV) was carried out using an EG&G model 273A potentiostat with a three-electrode cell using Pt for the working and counter electrodes and $Ag–Ag^+$ as a standard reference electrode. Solutions (*ca.* 10^{-3} mol dm^{-3}) were prepared in dry CH_2Cl_2 with 0.1 mol dm^{-3} NBu_4ClO_4 as the supporting electrolyte. They were purged with N_2 for 20 min prior to recording the CV traces.

For UV/VIS spectroelectrochemical studies, an optically transmitting thin-layer working electrode (OTTLE) made of platinum gauze (62% transmittance) was used with a platinum auxiliary electrode. For convenience, a silver wire was used as a pseudo-reference electrode. Resonance-Raman spectra were recorded in a cell fitted with an optically transmitting (but not thin-layer) platinum-gauze electrode, using an Ar^+ laser as excitation source in a backscattering geometry with a liquid-nitrogen cooled charge coupled device (CCD) multichannel array as the detector.[5,6]

The UV/VIS absorption spectra of both the ground-state and electrochemically reduced complex were recorded using a diode-array spectrophotometer (Hewlett-Packard model 8452A).

The set-up for flash photolysis has also been described.[5] Briefly, an Nd/YAG pulsed laser (pulse duration 8–10 ns) with harmonic outputs at 532 and 355 nm was used. Transient changes in absorbance were monitored with a pulsed xenon-arc source and a dual diode-array multichannel detector.

Molecular orbital calculations were carried out with HYPERCHEM[7] modelling software using an IBM personal computer. As a first approximation, calculations were carried out not on the metal complex but on free dpq. In order to generate a structure for free dpq suitable for these calculations two approaches are possible. The first is to use the geometry available from the X-ray data on the complex [after removing the metal centre and the other (phosphorus) ligands and counter ions]. The second approach is to optimise the geometry of the ligands using a semiempirical method. The latter gives a structure with inter-ring torsion angles which are too large ($\approx 90°$) but has the advantage that it could in principle be used to generate a reasonable geometry for the ligand radical anion which is not available from X-ray data. The geometry of the neutral dpq obtained from AM1 calculations[8] with the inter-ring torsions constrained to 30° is similar to that of the ligand in the complex as shown by the X-ray analysis (bond lengths agree within 0.01 Å in most cases, with a maximum error of ±0.03 Å) but has a symmetrical quinoxaline ring. The AM1 calculations of the molecular orbitals were carried out using this geometry.

† *Non-SI unit employed:* eV ≈ 1.60×10^{-19} J.

Table 1 Atomic coordinates for complex **1**

Atom	*x*	*y*	*z*	Atom	*x*	*y*	*z*
Cu(2)	2177(1)	−3193(1)	3329(1)	C(50)	2558(6)	427(6)	3333(5)
Cu(1)	1691(1)	121(1)	1681(1)	C(51)	2657(8)	−66(7)	3814(5)
P(1)	1850(1)	305(2)	687(1)	C(52)	2190(9)	−445(7)	4094(6)
P(2)	1808(1)	1031(2)	2407(1)	C(53)	1598(7)	−334(7)	3912(5)
P(3)	2582(1)	−3945(2)	2593(1)	C(54)	1480(6)	147(6)	3409(5)
P(4)	2373(1)	−3402(1)	4318(1)	C(55)	2635(4)	−3376(5)	1904(4)
N(3)	1236(3)	−3057(4)	3216(3)	C(56)	3172(5)	−3145(6)	1646(5)
N(4)	2141(3)	−2099(4)	2926(3)	C(57)	3187(6)	−2653(7)	1166(6)
N(1)	829(3)	−407(4)	1816(3)	C(58)	2644(8)	−2408(7)	910(5)
N(2)	1950(3)	−889(4)	2120(3)	C(59)	2100(7)	−2629(6)	1145(5)
C(18)	827(5)	−3480(6)	3500(5)	C(60)	2088(5)	−3117(5)	1648(4)
C(17)	257(5)	−3204(7)	3663(5)	C(61)	3342(4)	−4371(6)	2718(5)
C(16)	117(5)	−2428(7)	3547(5)	C(62)	3710(5)	−4077(6)	3176(5)
C(15)	526(5)	−1992(6)	3250(5)	C(63)	4273(6)	−4409(8)	3315(6)
C(14)	1073(4)	−2324(5)	3070(4)	C(64)	4455(6)	−5043(9)	3005(8)
C(13)	1573(4)	−1899(5)	2760(4)	C(65)	4119(7)	−5335(8)	2548(8)
C(12)	2624(4)	−1708(5)	2705(4)	C(66)	3550(6)	−5000(7)	2411(6)
C(11)	3229(4)	−1907(6)	2865(4)	C(67)	2094(4)	−4761(5)	2385(5)
C(10)	3707(5)	−1488(7)	2660(5)	C(68)	1994(6)	−4990(7)	1789(5)
C(9)	3609(4)	−823(6)	2300(5)	C(69)	1618(8)	−5617(8)	1658(7)
C(8)	3038(4)	−619(6)	2138(4)	C(70)	1373(8)	−6019(8)	2118(9)
C(7)	2527(4)	−1052(5)	2327(4)	C(71)	1464(6)	−5805(7)	2693(8)
C(6)	1479(4)	−1311(5)	2315(4)	C(72)	1844(5)	−5180(7)	2834(6)
C(5)	887(4)	−1133(6)	2012(4)	C(73)	1826(5)	−3012(6)	4858(5)
C(4)	449(4)	−1678(6)	1880(4)	C(74)	1447(5)	−2429(6)	4702(5)
C(3)	−71(5)	−1462(7)	1565(5)	C(75)	1060(6)	−2100(7)	5115(6)
C(2)	−148(5)	−720(7)	1386(5)	C(76)	1043(7)	−2367(8)	5691(7)
C(1)	306(5)	−215(6)	1513(5)	C(77)	1434(7)	−2950(9)	5872(6)
C(19)	1519(6)	−404(6)	160(4)	C(78)	1817(6)	−3272(8)	5465(6)
C(20)	1250(5)	−1045(7)	380(5)	C(79)	3115(5)	−3053(6)	4603(4)
C(21)	1045(6)	−1623(8)	−8(6)	C(80)	3275(5)	−2327(6)	4400(5)
C(22)	1117(9)	−1573(11)	−610(7)	C(81)	3813(6)	−1997(7)	4605(6)
C(23)	1403(11)	−921(12)	−838(7)	C(82)	4206(6)	−2406(10)	4987(6)
C(24)	1621(10)	−338(10)	−452(6)	C(83)	4020(7)	−3137(10)	5190(6)
C(25)	2652(5)	329(6)	429(4)	C(84)	3483(5)	−3444(7)	5000(5)
C(26)	2999(5)	−284(7)	626(5)	C(85)	2355(5)	−4445(6)	4418(4)
C(27)	3592(7)	−368(8)	443(6)	C(86)	2858(6)	−4891(6)	4292(4)
C(28)	3828(6)	170(11)	48(7)	C(87)	2796(8)	−5673(7)	4266(5)
C(29)	3480(6)	758(10)	−162(7)	C(88)	2273(10)	−6027(8)	4347(7)
C(30)	2878(6)	857(8)	29(5)	C(89)	1755(8)	−5585(9)	4485(6)
C(31)	1530(6)	1235(7)	482(4)	C(90)	1795(6)	−4797(7)	4530(5)
C(32)	1801(7)	1902(7)	681(5)	Cl(2)	−116(6)	−5184(7)	4557(5)
C(33)	1529(10)	2615(9)	581(7)	O(21)	−704(12)	−4964(19)	4298(13)
C(34)	988(13)	2690(12)	311(10)	O(22)	−204(9)	−5549(9)	5167(7)
C(35)	672(9)	2040(13)	134(9)	O(23)	220(14)	−5573(19)	4142(12)
C(36)	940(6)	1289(9)	189(6)	Cl(3)	4966(5)	−4995(6)	5192(3)
C(37)	1127(4)	1612(6)	2531(5)	O(31)	5507(10)	−4846(15)	4895(12)
C(38)	756(5)	1803(6)	2035(5)	O(32)	4860(11)	−4470(12)	5669(9)
C(39)	243(5)	2270(7)	2103(6)	O(33)	4946(12)	−5763(11)	5426(10)
C(40)	98(6)	2536(8)	2659(8)	O(34)	4417(10)	−4937(15)	4771(12)
C(41)	453(7)	2369(8)	3165(7)	Cl(1)	4861(2)	1374(2)	−1271(2)
C(42)	964(5)	1893(7)	3103(5)	O(11A)	4888(7)	645(7)	−985(7)
C(43)	2429(5)	1725(5)	2353(5)	O(12A)	4466(7)	1909(8)	−958(7)
C(44)	2435(6)	2389(7)	2687(6)	O(13A)	5477(6)	1706(8)	−1261(7)
C(45)	2919(9)	2901(9)	2644(7)	O(14A)	4680(7)	1316(8)	−1894(6)
C(46)	3408(8)	2735(9)	2293(9)	O(11B)	4861(15)	1607(18)	−667(9)
C(47)	3404(6)	2075(9)	1954(8)	O(12B)	4915(15)	522(11)	−1296(15)
C(48)	2918(5)	1573(7)	1980(6)	O(13B)	5343(12)	1676(17)	−1617(13)
C(49)	1966(5)	533(5)	3121(4)	O(14B)	4267(11)	1510(17)	−1543(15)

The ZINDO/S calculations[9] were carried out to determine the orbital origin of the observed UV/VIS absorption bands. There is some difficulty in choosing a suitable geometry for calculation on the radical anion. Geometry optimisation of the radical anion form using the same inter-ring torsion constraints as for the neutral dpq gave a structure with a shortened C–C inter-ring bond which is inconsistent with the Raman data (see below), while the X-ray data are only suitable for the neutral, co-ordinated dpq. However, the calculated UV/VIS transitions are not very sensitive to the ligand geometry since the spectra calculated using either of these two structures were closely comparable.

Crystallography

Crystal data for complex 1. $C_{90}H_{72}Cl_2Cu_2N_4O_8P_4$, M = 1659.4, monoclinic, space group $P2_1/a$, a = 21.787(10), b = 17.445(7), c = 22.083(7) Å, β = 90.55(3)°, U = 8393(6) Å^3, Z = 4, D_c = 1.313 Mg m^{-3}, $F(000)$ = 3424, λ(Mo-Kα) = 0.710 73 Å, μ = 0.70 mm^{-1}. Dark red hexagonal prisms, crystal size 0.21 × 0.24 × 0.66 mm, Siemens P3/V2000 diffractometer, θ–2θ scans, scan width 0.8°, scan range 2 < θ < 27.5°, 14 884 unique reflections measured, absorption correction, direct methods solution (SHELXS 86),[10] full-matrix least-squares refinement on F^2 (SHELXL 93),[11] non-hydrogen atoms anisotropic, hydrogens included at calculated positions.

In the final cycles 5270 data with $I > 3\sigma(I)$ were used to refine 963 parameters. Final $R = 0.082$, goodness of fit = 1.22. The atomic coordinates are listed in Table 1 and selected bond lengths and angles in Table 2. Complete atomic coordinates, thermal parameters, and bond lengths and angles have been deposited at the Cambridge Crystallographic Data Centre. See Instructions for Authors, *J. Chem. Soc., Dalton Trans.*, 1996, Issue 1.

Results and Discussion

The crystal structure of complex **1** is shown in Fig. 1. The two pyridine rings are twisted (by 31 and 33° respectively) with respect to the mean plane of the quinoxaline group, which is itself non-planar, the nitrogen-containing ring showing a slight twist conformation with respect to the benzo moiety [Fig. 1(*b*)]. Torsion angles are N(4)–C(12)–C(7)–N(2) −8.7, C(12)–C(7)–N(2)–C(6) +3.8, C(7)–N(2)–C(6)–C(13) +5.3, N(2)–C(6)–C(13)–N(4) −10.6, C(6)–C(13)–N(4)–C(12) +5.6 and C(13)–N(4)–C(12)–C(7) +3.6°. These effects are a consequence of the steric interference between the hydrogens of the pyridyl groups as relief of steric strain is achieved without any distortion of the bond lengths or interbond angles.

The cyclic voltammogram of complex **1** in CH_2Cl_2 solution presented in Fig. 2 shows a well defined single, reversible redox wave with $E_{\frac{1}{2}} = -0.9$ V *vs.* Ag^+–Ag. Reduction of the mononuclear complex **2** was quasi-reversible and spectroelectrochemical measurements on this species were not further pursued. Fig. 3(*b*) shows the spectral changes observed for **1** in the OTTLE cell [compared to the ground-state spectrum in Fig. 3(*c*)], with the potential held at −1.0 V *vs.* silver wire as reference. At this potential reduction of **1** proceeds to completion as marked by the growth in intensity of the UV/VIS band near 435 nm (ε_{max} *ca.* 6800 $dm^3\ mol^{-1}\ cm^{-1}$). The spectral changes were fully reversible. The spectrum is similar to the excited-state absorption spectrum of the mononuclear complex **2** in Fig. 3(*a*), recorded by flash photolysis using a multichannel diode array.[5] Thus the spectral changes in Fig. 3(*b*) are consistent with assignment to the $dpq^{\bullet -}$ radical anion and the species obtained upon electrochemical reduction of **1** can be formulated as $[(Ph_3P)_2Cu^I(dpq^{\bullet -})Cu^I(PPh_3)_2]^+$.

Resonance-Raman spectra of complex **1** and of the species present following one-electron reduction are presented in Fig. 4. The excitation wavelength, 488 nm, falls within the $\pi^* \longrightarrow \pi^*$ band of the radical anion [Fig. 3(*b*)] and, although appreciably away from λ_{max} for this species, high-quality spectra are observed. The 457 nm output of the Ar^+ laser is closer to λ_{max}, but fluorescence at this wavelength resulted in extremely noisy Raman signals. The most notable feature of Fig. 4 is the gain in intensity of the bands at 1594 and 1320 cm^{-1} upon reduction of **1**. The feature at 1594 cm^{-1} was also observed in the *transient* (*i.e.* power-resolved) resonance-Raman spectra of **1** reported in our earlier paper.[4] This is consistent with the conclusion drawn earlier that the radical anion $dpq^{\bullet -}$ is present under the conditions of both electrochemical reduction and pulsed laser photoexcitation.

The resonance-Raman spectra for the neutral complex **1** closely resemble those reported in a study[12] of the binuclear ruthenium(II) complex with the same dpq ligand, where it was concluded that the vibrational modes are mainly localised on the quinoxaline part of the ligand, based on a comparison with surface-enhanced Raman spectra of dpq. The study found no

Table 2 Selected bond lengths (Å) and angles (°) for complex **1**

Cu(1)–N(1)	2.114(8)	C(2)–C(3)	1.36(2)
Cu(1)–N(2)	2.087(7)	C(3)–C(4)	1.376(14)
Cu(1)–P(1)	2.248(3)	C(4)–C(5)	1.377(12)
Cu(1)–P(2)	2.269(3)	C(5)–C(6)	1.482(12)
Cu(2)–N(3)	2.076(7)	C(6)–C(13)	1.434(11)
Cu(2)–N(4)	2.106(7)	C(7)–C(8)	1.414(12)
Cu(2)–P(3)	2.272(3)	C(7)–C(12)	1.430(11)
Cu(2)–P(4)	2.251(3)	C(8)–C(9)	1.338(12)
N(1)–C(1)	1.359(11)	C(9)–C(10)	1.422(13)
N(1)–C(5)	1.342(11)	C(10)–C(11)	1.354(13)
N(2)–C(6)	1.336(10)	C(11)–C(12)	1.404(12)
N(2)–C(7)	1.363(10)	C(13)–C(14)	1.489(12)
N(3)–C(14)	1.364(11)	C(14)–C(15)	1.388(12)
N(3)–C(18)	1.320(11)	C(15)–C(16)	1.347(13)
N(4)–C(12)	1.351(10)	C(16)–C(17)	1.410(14)
N(4)–C(13)	1.333(10)	C(17)–C(18)	1.383(13)
C(1)–C(2)	1.351(14)		
N(1)–Cu(1)–N(2)	78.6(3)	Cu(2)–N(4)–C(12)	125.8(6)
N(1)–Cu(1)–P(1)	110.2(2)	Cu(2)–N(4)–C(13)	112.6(6)
N(1)–Cu(1)–P(2)	107.4(2)	C(12)–N(4)–C(13)	119.5(7)
N(2)–Cu(1)–P(1)	122.1(2)	N(1)–C(5)–C(4)	121.4(9)
N(2)–Cu(1)–P(2)	103.6(2)	N(1)–C(5)–C(6)	114.9(8)
P(1)–Cu(1)–P(2)	124.90(11)	C(4)–C(5)–C(6)	123.4(9)
N(3)–Cu(2)–N(4)	79.2(3)	N(2)–C(6)–C(5)	114.0(7)
N(3)–Cu(2)–P(3)	111.8(2)	N(2)–C(6)–C(13)	120.7(8)
N(3)–Cu(2)–P(4)	108.2(2)	C(5)–C(6)–C(13)	125.3(8)
N(4)–Cu(2)–P(3)	103.6(2)	N(2)–C(7)–C(8)	121.1(8)
N(4)–Cu(2)–P(4)	124.2(2)	N(2)–C(7)–C(12)	119.6(8)
P(3)–Cu(2)–P(4)	121.94(11)	C(8)–C(7)–C(12)	119.1(8)
Cu(1)–N(1)–C(1)	124.4(7)	N(4)–C(12)–C(7)	120.2(8)
Cu(1)–N(1)–C(5)	112.1(6)	N(4)–C(12)–C(11)	121.2(8)
C(1)–N(1)–C(5)	117.8(8)	C(7)–C(12)–C(11)	118.6(8)
Cu(1)–N(2)–C(6)	114.2(6)	N(4)–C(13)–C(6)	120.1(8)
Cu(1)–N(2)–C(7)	125.2(6)	N(4)–C(13)–C(14)	115.0(7)
C(6)–N(2)–C(7)	119.0(7)	C(6)–C(13)–C(14)	124.9(8)
Cu(2)–N(3)–C(14)	112.9(6)	N(3)–C(14)–C(13)	112.7(8)
Cu(2)–N(3)–C(18)	123.4(7)	N(3)–C(14)–C(15)	123.1(8)
C(14)–N(3)–C(18)	117.5(8)	C(13)–C(14)–C(15)	123.9(8)

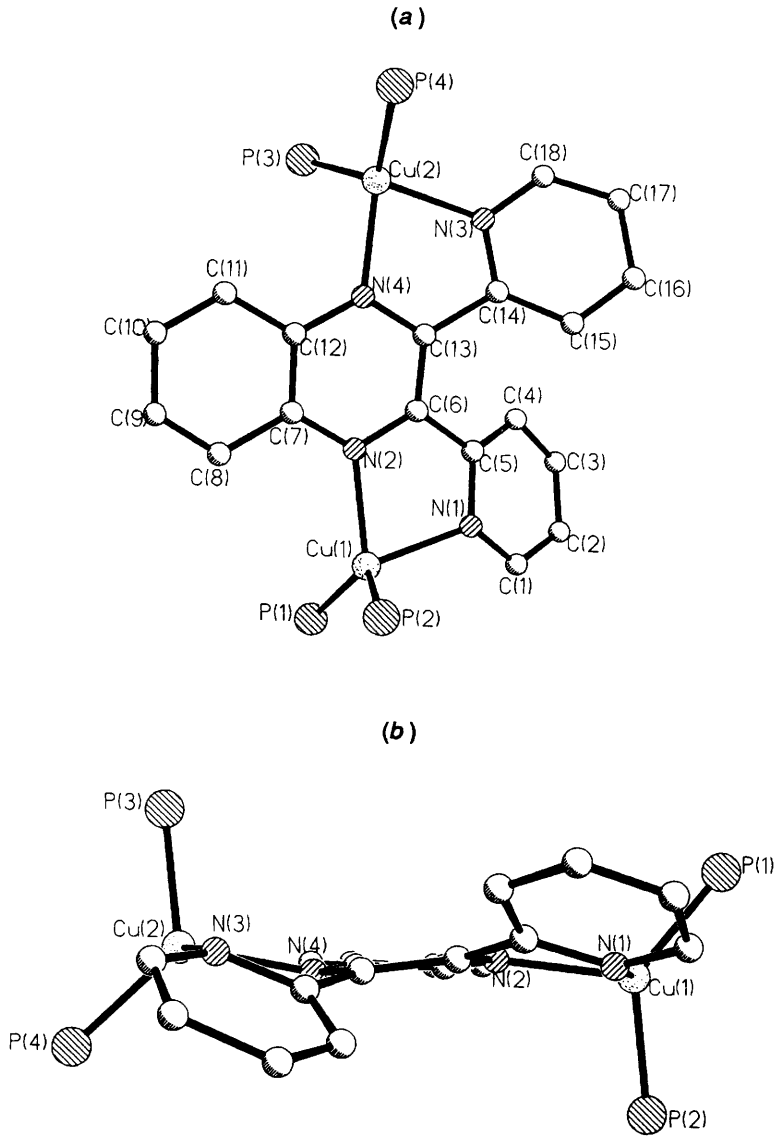

Fig. 1 Crystal structure of complex **1**: (*a*) top view; (*b*) side view. The six phenyl groups have been omitted for clarity

resonance-Raman evidence for $dpq^{\bullet -}$ -centred modes when the complex was electrochemically reduced. However, the investigations were only carried out at one excitation wavelength, 514.5 nm, which is appreciably removed from the maximum of the radical anion absorption. The explanation suggested in the latter study for the absence of resonance-Raman features due to $dpq^{\bullet -}$ was that the radical anion-centred $\pi^* \longrightarrow \pi^*$ transition, taken to be from the bridging ligand LUMO (lowest unoccupied molecular orbital) to LUMO + 1, involved only minor excited-state geometry changes. No computational data were available to support this proposal. Semiempirical MO calculations carried out here on neutral dpq, using either AM1 or ZINDO methods and parametrisation, both give a LUMO and LUMO + 1 which are very close in energy. The next lowest-lying orbital is > 1 eV above this pair. Contour plots of the orbital density of the HOMO (highest occupied molecular orbital), LUMO and LUMO + 1 calculated using AM1 are shown in Fig. 5. The energy ordering of the two lowest-lying unoccupied orbitals is reversed when ZINDO/S calculations are carried out so that it is not possible reliably to predict which one of these orbitals actually lies lower, using semiempirical methods. Moreover, both sets of calculations were carried out in the absence of the metal centres and take no account of the possible influence of these on the orbital energy order. Experimental data are required to decide this point.

The small energy gap between LUMO and LUMO + 1 is reflected in the long wavelength (> 1500 nm) of the lowest-energy transition calculated (using ZINDO/S) for the UV/VIS spectrum of the radical anion. The absorption-band envelope in the visible region can be assigned to transitions involving promotion from the LUMO to LUMO + 2 up to LUMO + 6 (where the LUMO is the lowest unoccupied orbital in the neutral species and is singly occupied in the radical). Considerable resonance-Raman enhancement of vibrational modes of the radical anion would therefore be expected, since significant changes in bonding should accompany the transitions in the visible region. This is in agreement with our observations.

The frequency of the inter-ring ν(C–C) band in the resonance-Raman spectra of metal–bipyridine, –bipyrazine and –pyridylpyrazine complexes is known to fall in the range 1300–1350 cm^{-1} for the neutral complexes and shifts to higher wavenumbers in the spectra of the corresponding radical-anion form in each case. This is consistent with shortening of this C–C bond, reflecting an increase in the π-bond order accompanying one-electron reduction. The data for several such systems are summarised in Table 3. The strong resonance-Raman band at 1320 cm^{-1} for the neutral form of complex **1** can also reasonably be assigned to the inter-ring ν(C–C) stretch mode [C(6)–C(5) and C(13)–C(14) bonds, Fig. 1]. It is striking, however, that in this case, although the spectra of the radical anion of **1** clearly show that the band at 1320 cm^{-1} is enhanced, as expected on the

basis of the above discussion on the transition involved, no shift in its position is observed. This suggests little or no change in the bond order of this particular bond in the radical anion compared to the neutral ground state. It might appear that the constraints arising from steric interference between the hydrogens of the pyridyl groups which force the pyridyl and quinoxaline rings to be non-planar in the ground-state complex (see above) continue to act so as to minimise the shortening of the C–C bond expected to accompany one-electron reduction. However, the MO calculations show that there are two candidates for the orbital which contains the unpaired electron in the radical. One of these, shown as the LUMO in Fig. 5, has bonding character between the pyridyl and quinoxaline rings and indeed is superficially very similar to the orbital which gives rise to the 45 cm^{-1} shift for the reduced form of 2,2′-bipyridyl (Table 3). The other possible candidate (shown as LUMO + 1) has little bonding character across this particular bond so that the change in bond order and associated wavenumber shift upon reduction arising from population of this orbital would be expected to be very much less.

The electrochemical and resonance-Raman data reported here and the transient UV/VIS and Raman spectra reported previously[4] are sufficiently similar that the m.l.c.t. state can be readily assigned as containing a singly reduced dpq ligand. The broad visible absorption band observed in both types of experiment is due to $\pi^* \longrightarrow \pi^*$ transitions of this radical anion centre. The transition from LUMO to LUMO + 1 of the radical is not expected to lie in the visible region, however, because the energy gap between these two orbitals is rather small and would correspond to a transition in the near-IR region. The $\pi^* \longrightarrow \pi^*$ absorption in the visible region would be expected to give resonance enhancement of dpq$^-$ radical anion modes through 'A-term' scattering. The negligible shift in the inter-ring stretching vibration observed upon reduction implies that the orbital in which the unpaired electron resides is essentially non-bonding between the rings. As the above calculations indicate, one of the two orbitals which are candidates for the singly occupied HOMO in the radical anion is indeed non-bonding between the rings while the second has considerable bonding character. The resonance-Raman evidence suggests that it is the former which is singly occupied in the radical species.

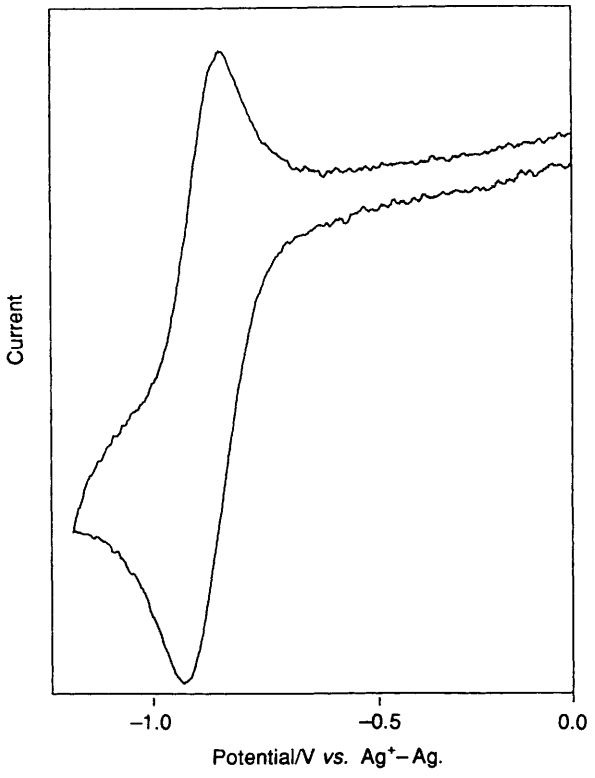

Fig. 2 Cyclic voltammogram of [**1**] in dry CH_2Cl_2 (*ca.* 10^{-3} mol dm^{-3}) Pt working and counter electrodes; Ag/Ag^+ reference. Scan rate 100 mVs^{-1}. Solution purged with N_2 for 20 minutes prior to recording CV

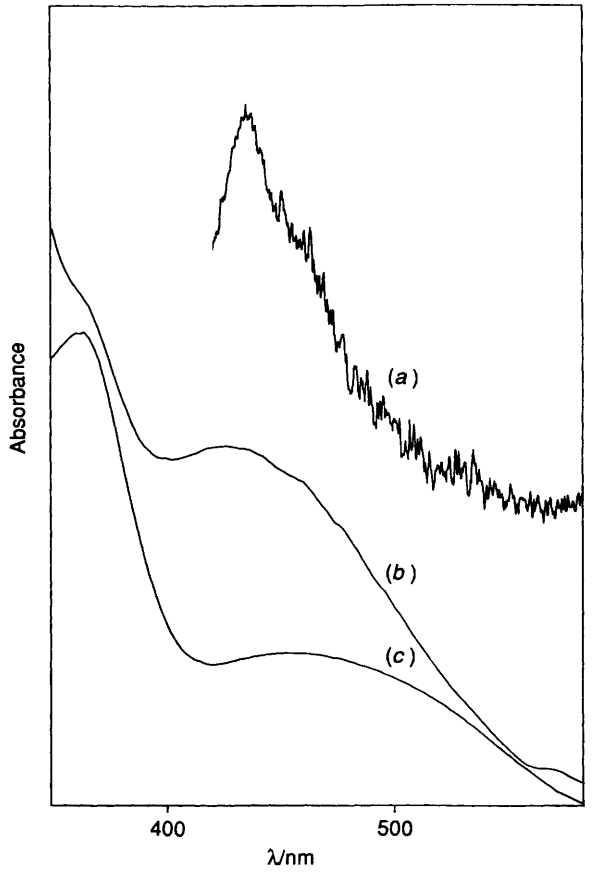

Fig. 3 Comparative ground-state and dpq$^{\bullet -}$ radical anion absorption spectra for complex **1**: (*a*) excited-state absorbance difference spectrum of dpq$^{\bullet -}$ recorded using a gated diode array (gate width 4 ns) 25 ns after pulsed laser excitation of **1** in CH_2Cl_2 (10^{-3} mol dm^{-3}) at 355 nm (laser pulse energy *ca.* 10 mJ), spectral accumulation 300 1s scans, slit width 50 μm; (*b*) reversible change in UV/VIS spectrum of a 10^{-3} mol dm^{-3} solution of **1** in CH_2Cl_2 recorded in an OTTLE cell during electrochemical reduction (measured potential, −1.0 V *vs.* silver wire, takes no account of internal resistance of the OTTLE cell); (*c*) UV/VIS spectrum of the solution of **1** used to record trace (*a*)

Table 3 Comparisons between inter-ring C=C stretching modes (cm^{-1}) for neutral and one-electron-reduced polypyridyl ligands

		ν_{CC}			
Complex	Ligand	neutral	reduced	Δ/cm^{-1}	Ref.
$[\{W(CO)_5\}_2(bipy')]$	4,4′-Bipyridyl	1300	1350	50	6
$[Ru(bipy)_3]^{2+}$	2,2′-Bipyridyl	1320	1365	45	13
$[Ru(bpyz)_3]^{2+}$	2,2′-Bipyrazine	1347	1359	12	14
$[Ru(ppyz)_3]^{2+}$	2-(2-Pyridyl)pyrazine	1335	1355	20	14
1	dpq	1320	1320	0	This work

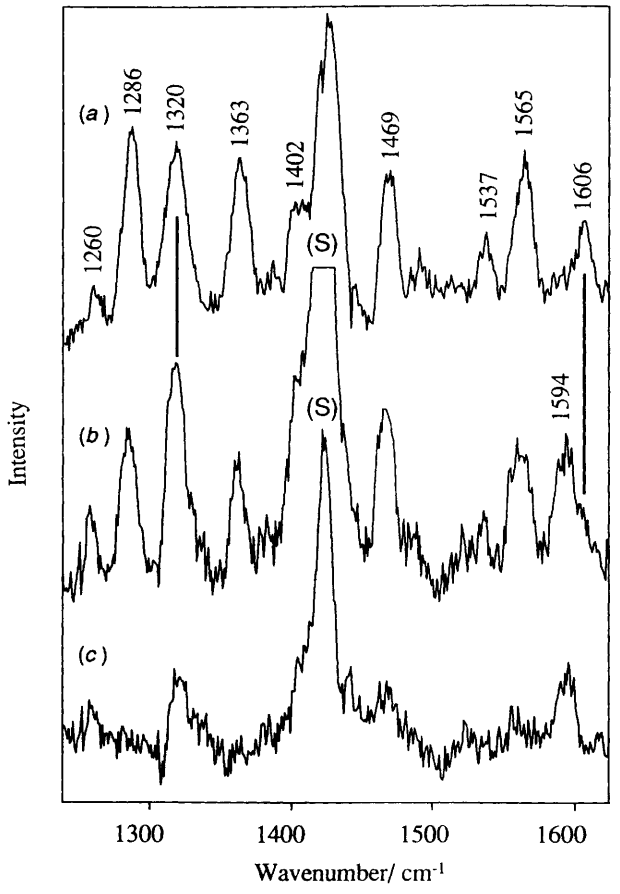

Fig. 4 Resonance-Raman spectra of complex **1** in dry CH_2Cl_2 (10^{-3} mol dm^{-3}) in a cell fitted with an optically transparent (but not thin-layer) electrode recorded at λ_{exc} = 488 nm at zero potential (*a*) and −1.0 V *vs.* silver wire (*b*); trace (*c*), *ie.* (*b*) − (*a*), is the difference spectrum. Spectral accumulation 20 × 20 s scans; slit width 5 cm^{-1}; laser power at sample *ca.* 30 mW. S = Solvent peak

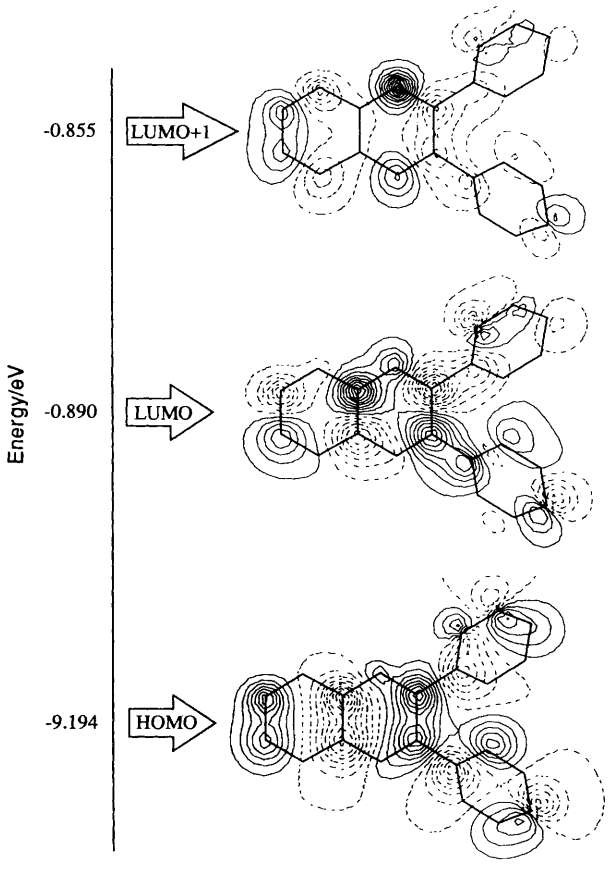

Fig. 5 Orbital density-contour plots for neutral dpq (geometry optimised by AM1). Contour plots shown at 0.5 Å above the quinoxaline plane. The pyridyl rings are out of plane; see Fig. 1(*b*)

Acknowledgements

We thank the EPSRC for support (Grant J/01905) and the School of Chemistry, Q. U. B., for a Research Studentship (to P. M. J.).

References

1 D. R. McMillin, J. R. Kirchoff and K. V. Goodwin, *Coord. Chem. Rev.*, 1985, **64**, 83.
2 K. C. Gordon and J. J. McGarvey, *Inorg. Chem.*, 1991, **30**, 2986.
3 V. Wing-Wah Yam and K. Kam-Wing Lo, *J. Chem. Soc. Dalton Trans.*, 1995, 499.
4 K. C. Gordon and J. J. McGarvey, *Chem. Phys. Lett.*, 1990, **173**, 443.
5 A. H. R. Al-Obaidi, K. C. Gordon, J. J. McGarvey, S. E. J. Bell and J. Grimshaw, *J. Phys. Chem.*, 1993, **97**, 10942.
6 R. A. McNicholl, J. J. McGarvey, A. H. R. Al-Obaidi, S. E. J. Bell, P. M. Jayaweera and C. G. Coates, *J. Phys. Chem.*, 1995, **99**, 12268.
7 HYPERCHEM, Autodesk Ltd., Sausalito, CA, 1993.
8 AMI Austin Method 1; M. J. S. Dewar, E. G. Zoebisch, E. F. Healy and J. J. P. Stewart, *J. Am. Chem. Soc.*, 1985, **107**, 3902.
9 ZINDO/S: Intermediate neglect of differential overlap method for spectroscopic investigations due to Zerner; J. E. Ridley and M. C. Zerner, *Theor. Chim. Acta*, 1976, **42**, 223.
10 G. M. Sheldrick, SHELXS 86, University of Göttingen, 1986.
11 G. M. Sheldrick, SHELXL 93, University of Göttingen, 1993.
12 J. B. Cooper, D. B. McQueen, J. D. Petersen and D. W. Wertz, *Inorg. Chem.*, 1990, **29**, 3701.
13 D. P. Strommen, P. K. Mallick, G. D. Danzer, R. S. Lumpkin and J. R. Kincaid, *J. Phys. Chem.*, 1990, **94**, 1357.
14 G. D. Danzer, J. A. Golus and J. R. Kincaid, *J. Am. Chem. Soc.*, 1993, **115**, 8643.

Received 19*th November* 1995; *Paper* 5/06198I